

The Impact of using Rice Husk Ash, Seawater and Sea Sand on Corrosion of Reinforcing Bar in Concrete

Dahlia Patah*, Amry Dasar

Department of Civil Engineering, Universitas Sulawesi Barat, Majene, INDONESIA

Jalan Prof. Dr. Baharuddin Lopa, SH, Talumung, Majene

*Corresponding author: dahliapatah@unsulbar.ac.id

SUBMITTED 02 November 2022 REVISED 09 May 2023 ACCEPTED 13 May 2023

ABSTRACT As infrastructure development continues to increase around the world, availability of river sand and tap water for making concrete are in potentially serious shortage, especially in coastal areas. To solve this problem, in the last decade researchers starts to investigate the potential of utilization seawater and sea sand as option for sustainable in concrete production. In different situations, Rice Husk Ash (RHA) is an agricultural industrial solid dreg in fine powder obtained from the combustion process. RHA which is generated from the combustion process of the husk either natural or artificial is considered a severe solid waste to the environment. RHA with potential pozzolanic for alternative and sustainable material for partial substitution of cement to improve concrete durable and strength and, simultaneously, to diminish potential of corrosion in consequence of the harsh environment situations. RHA is potentially used as a kind SCM (supplementary cementitious material) because high pozzolanic activity with correspond to a large amount of silica. The aim of this study is to investigate the impact of seawater for mixing, sea sand and substitution ratio of RHA on the corrosion of reinforcing bar. The specimen measured 150 mm in thick, with rectangular areas of 400 x 400 mm and plain steel bars with diameter of 10 mm were embedded. The specimen was evaluated by half-cell potential (HCP) and hammer test for corrosion and concrete quality, respectively. The result of this study showed all specimens mixed with seawater, river sand and replacement ratio of rice husk ash for RHA-0%, RHA-5%, RHA-10% and RHA-15% were estimated to be corroded by the half-cell potential method and be consistent with the result of actual corrosion. Meanwhile, only the specimen mixed with tap water, sea sand and the addition of 5% RHA was effectively resisted to corrosion which was similar with normal concrete.

KEYWORDS Concrete; Sea Sand; Corrosion; Half-Cell Potential; Actual Corrosion.

© The Author(s) 2023. This article is distributed under a Creative Commons Attribution-ShareAlike 4.0 International license.

1 INTRODUCTION

Cement is the most widely used building material in the construction industry and accounts for approximately 8% of global carbon dioxide (CO₂) emissions (Fapohunda et al., 2017). The most common type of cement used for building construction is Ordinary Portland Cement (OPC) due to its widespread importance. However, several attempts have been conducted to improve the performance and sustainability of OPC, with focus on enhancing its strength, corrosion resistance, and environmental impact. Given the significant energy requirements involved in OPC production, finding a suitable replacement is important (Henry and Lynam, 2020).

Rice husks, which are widely available in many countries, contain approximately 20% grain. Af-

ter harvesting the coarse grain (paddy), the next step involves hulling to separate rice from husks. The advantage is that the process of extracting rice from husks does not require separate transportation for the fields. In addition to being valuable as animal feed, rice husks are not easily composted (Bui, 2001). When rice husks are burned at high temperatures, approximately 20% of their ash (RHA) is produced. RHA, rich in amorphous silica, is an alternative to pozzolan or cement. Crystalline silica, found in minor amounts, does not exhibit a significant pozzolanic reaction with Ca(OH₂) (Nguyen et al., 2011). The classification of RHA depends on the content of amorphous SiO₂, which is influenced by burning time and degree, as well as thermal treatment conditions (Bui, 2001). Burning temperatures below 750°C often

result in reactive amorphous RHA, as reported by studies on various similar scenarios (Boateng and Skeete, 1990). RHA is a pozzolan ingredient comprising a minimum of 70% silicon dioxide, aluminium, and iron oxide. The amorphous SiO_2 content and the permeable structure of RHA depend on the burning degree and duration of rice husks (Van Tuan et al., 2011). RHA can also contain as much as 80 to 85% highly reactive silica (Kishore et al., 2011). Gursel et al. (2016) stated that silica contents in RHA range from 90 to 95%. Several studies have assessed impact of replacing OPC with RHA based on the compressive strength, corrosion resistance, and level of porosity in concrete for over 20 years (Bui, 2001; Boateng and Skeete, 1990; Kishore et al., 2011; Gursel et al., 2016; Fapohunda et al., 2017; Van Tuan et al., 2011). Based on the mechanical properties evaluated by Patah and Dasar (2022), RHA positively contributed to concrete strength, where the compressive strength of RHA concrete (RHA-7.5) was relatively 48.79 MPa, while normal concrete (RHA-0) was 45.30 MPa.

The availability of rice husks and the pozzolanic properties of its ash indicates the necessity for a comprehensive evaluation of the partial substitution of OPC with RHA. In circumstances where the evaluation is performed effectively, environmental pollution resulting from the manufacturing of OPC could be potentially reduced. However, in terms of energy content, RHA has been predicted to offer approximately 26 MJ per kg of usable energy generated, surpassing the energy consumption of 4.6 MJ to 6.4 MJ per kg of cement binder production (Henry and Lynam, 2020; Hammond and Jones, 2008; Reddy and Jagadish, 2003).

Currently, most of the existing study focuses on the effect of using seawater mixed or unwashed sea sand in concrete. However, limited investigations have been carried out on the combined impact of using seawater mixed with unsalted sea sand on concrete properties. It is widely acknowledged that unlike tap water, seawater, due to its chemical composition, tends to affect the performance of cement-based composites significantly. The presence of chemicals in seawater can interfere with the cement properties, such as setting and rheology, and also influences the mechanical strength and durability of concrete. Using tap water for concrete mixing is not environmentally

preferable in dry areas. By substituting tap water with seawater in concrete mixing, it would be possible to minimize energy consumption as well as conserve precious resources.

Previous studies have investigated the use of seawater and sea sand in the mixing of concrete, particularly examining corrosion evaluation and impact of seawater on concrete properties. These investigations have consistently proven that the incorporation of seawater in concrete leads to enhanced compressive strength and durability against reinforcing steel corrosion compared to concrete mixed with tap water (Dasar et al., 2013, 2016, 2020). Several studies reported that various chemical agents in seawater can increase concrete strength at an early age, yielding comparable or even higher results than concrete produced with tap water (Fu et al., 2020; Li et al., 2015). The chloride ions present in seawater facilitated cement hydration, thereby resulting in reduced setting time (Yu et al., 2017) and accelerated hardening (Sikora, 2020*b,a*; Li et al., 2020). Additionally, it was observed that the adsorption performance of concrete with seawater decreases as the porosity of concrete reduces (Sikora, 2020*b,a*; Etxeberria et al., 2016). Regarding the use of unwashed sea sand, preliminary studies reported that it could influence the performance of cement-based composites, particularly in two significant aspects, such as the presence of salt agents and its physical properties (Wang et al., 2017; Ting et al., 2020).

This study aims to determine the effect of RHA, seawater, and sea sand on the durability of concrete. The results obtained provide valuable guidelines for subsequent studies and the practical application of cement composites made from RHA in conjunction with seawater or sea sand.

2 METHODS

2.1 Material

The kind of cement used in this study is Portland Composite Cement (PCC) Type I based on SNI 15-7064-2004. It is commonly produced by an Indonesian cement factory and readily accessible in the market. Rice husks ash (RHA) was used as a partial replacement for PCC cement. Rice husks used were from Wonomulyo Regency, West Sulawesi Province, Indonesia. The dried RHA was



Figure 1 Appearance of RHA

sieved using a No. 50 sieve, as shown in Figure 1. The chemical properties of both PCC and RHA are also shown in Table 1. Two types of water were used in this study, tap water obtained from the laboratory and seawater collected from Barane Beach, Majene Regency, West Sulawesi Province, Indonesia. Furthermore, two types of fine aggregate or sand were used, namely washed sea sand and river sand. Both sands were filtered using a 5 mm sieve. Sea sand obtained from Pamboang Beach, Majene Regency, was used without undergoing a desalting process. Coarse aggregate or gravel used had a maximum size of 20 mm and was sourced from the Laliko River. The properties of the materials used are shown in Table 2. The classification limits for sand and gravel are in accordance with SNI 03-1968-1990. The properties of sand and gravel are shown in Table 3. The fineness modulus (FM) of the unwashed sea sand is finer compared to the river sand.

2.2 Mix Proportion and Specimen Design

In this study, a total of eight variations of concrete were produced, while four specimens were prepared using seawater mixed with river sand and

Table 1. Chemical properties of PCC and RHA

No.	Chemical composition	PCC, %	RHA, %
1	SiO ₂	20.5	93.61
2	Al ₂ O ₃	5.5	-
3	Fe ₂ O ₃	3.9	0.292
4	CaO	62	0.7
5	MgO	0.89	-
6	SO ₃	2.8	-
7	K ₂ O	-	3.52

Table 2. Properties of material used

Material	Properties	Specific gravity (g cm ⁻³)	Specific surface area (m ² g ⁻¹)
Cement, C	PCC Type 1	3.15	382
RHA	Passing sieve No.50	2.24	87
Fine Aggregate :		2.13	
- River Sand	Passing sieve 5 mm		-
- Sea Sand		2.61	
Coarse Aggregate	Maximum 20 mm	2.56	-
Water:		1	
- Tap Water	-		-
- Sea Water		1.03	

Table 3. Physical properties of aggregates used

Properties	Fine aggregate		Coarse aggregate
	River sand	Sea sand	
Sludge levels, %	0.49	0.6	0.55
Specific gravity, gm ⁻³	2.46	2.61	2.62
Water content, %	7.22	10.88	0.64
Organic level	No.2	No.2	No.2
Water absorption, %	1.69	1.75	0.64
Fineness modulus	3.39	2.77	7.82

different quantities of RHA as a substitute for cement. Additionally, four other specimens were prepared using tap water mixed with sea sand and varying quantities of RHA. RHA of 0%, 5%, 10% and 15% by weight of cement was used as a cement substitute. The design and number of specimens used are shown in Table 4. The specimens are prism-shaped with dimensions of 40x40x15cm, and each was fitted with a total of 4 plain round steel bars 10 mm and 100 mm in diameter and length, respectively. The depths of concrete covers were 20, 30, 40, and 50 mm from the surface, with

Table 4. Design and number of concrete specimens

Specimen code	Fine aggregate	RHA percentage	Mixing	Number of specimens
PS-ASP0-AL	River sand	0%	Seawater	1
PS-ASP5-AL	River sand	5%	Seawater	1
PS-ASP10-AL	River sand	10%	Seawater	1
PS-ASP15-AL	River sand	15%	Seawater	1
PP-ASP0-AT	Sea sand	0%	Tap water	1
PP-ASP5-AT	Sea sand	5%	Tap water	1
PP-ASP10-AT	Sea sand	10%	Tap water	1
PP-ASP15-AT	Sea sand	15%	Tap water	1

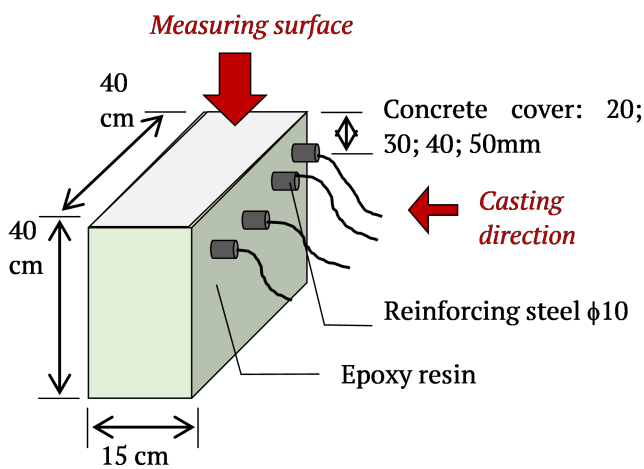


Figure 2 Design and shape of the specimen

the current study focusing specifically on specimens with a 20mm concrete cover for evaluating the embedded reinforcing bars. The epoxy-type resin was applied to five surfaces of concrete prism specimens, while one surface remained uncoated for measurement purposes (Figure 2). A cable was connected to reinforcing steel to measure corrosion. A water-to-binder (w/b) ratio of 0.5 was used, and all concrete was mixed according to the procedure in Figure 3. After casting, all specimens were stored for 24 hours in a laboratory room where the room temperature was not controlled. After 24 hours of curing, the test specimen was moulded, and concrete was stored under the same curing conditions for different test ages.

2.3 Test Method

2.3.1 Half-Cell Potential (HCP)

The HCP technique was used to estimate the risk of possible corrosion of reinforcing bars in concrete structures. In order to minimize fluctuations in the HCP value, a pre-wetting process was carried out before testing. This involves placing a wet cloth on the measurement surface of concrete specimen for 30 minutes. During the HCP test, the measurement was taken three times, and the average of these measurements was recorded as actual value. The HCP was measured using a multimeter (Avometer Digital Zotek ZT112) and a reference electrode (Professional 112 Type Silver/Silver Chloride) made of Ag/AgCl which was connected to the specimen (Figure 4). The HCP values obtained were then compared to a threshold value specified in the ASTM C876-15 standard. According to the provided information, when the value was less than -256 mV, there was a 90% chance that reinforcing bars had already corroded, as shown in Table 5. The HCP measurements were conducted at regular intervals, from the age of 1 day and continued up to 189 days. The measurements were halted as soon as corrosion in reinforcing bars embedded in concrete was detected.

2.3.2 Hammer Test

The hammer test was performed at 189 days based on the SNI-03-4430-1997 standard. Its purpose was to assess the compressive strength of the specimen after detecting corrosion based on the HCP result. Prior to conducting the test, concrete surface was levelled. For the hammer test, an HT-225 concrete Rebound Hammer was used. The test was

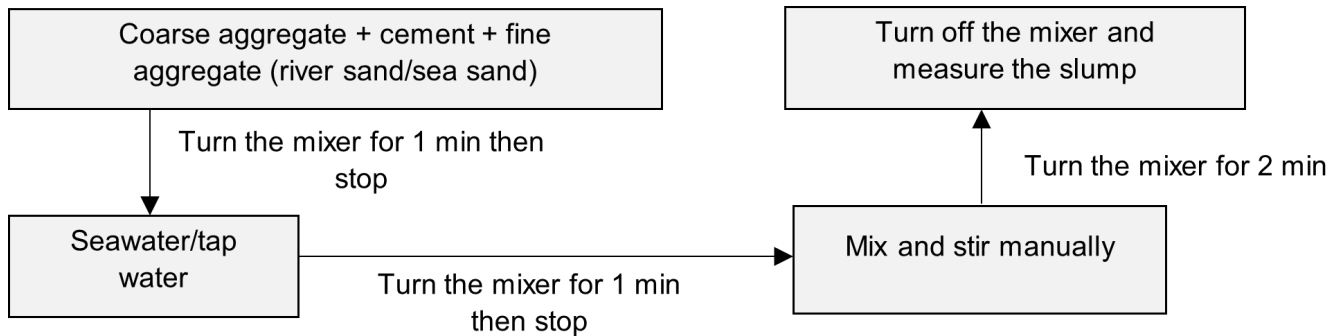


Figure 3 Concrete mixing procedure

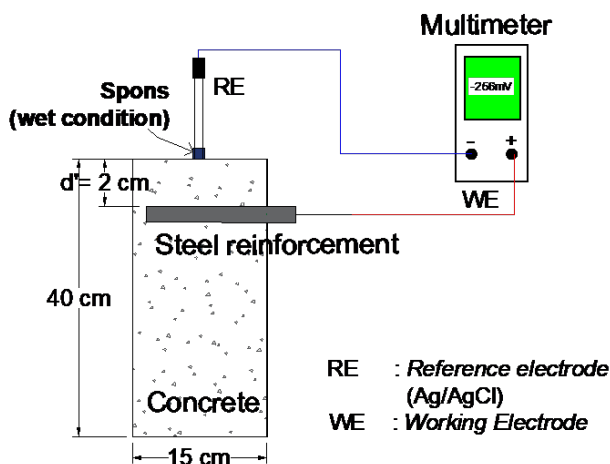


Figure 4 Thr HCP measurement scheme

conducted on a 40x40 cm width of concrete specimen, at 90° angles, and 10 measurements were taken at points spaced 5 cm apart along the surface. These measurements were recorded, and the average value was calculated. The corrected value was also determined according to the instrument calibration factor. After the rebound values were obtained, a vertical line was drawn, as shown in Figure 5. This represents the relationship between concrete compressive strength and the reflected value on the hammer dial based on the degree of the test performed.

2.3.3 Actual Corrosion

In order to accurately assess the level of corrosion in the embedded reinforcing bars within concrete (concrete cover thickness of 20 mm), a visual inspection is performed. This involves the extrac-

Table 5. Corrosion probability (ASTM C876, 2015)

HCP (mV)		Corrosion activity
Ag/AgCl	Cu/Cu(SO) ₄	
> - 106	> -200	10% corrosion risk (low)
-106 to -256	-200 to -350	50% corrosion risk (medium)
< - 256	< - 350	> 90% corrosion risk (high)
< - 406	< - 500	100% corrosion (Very high)

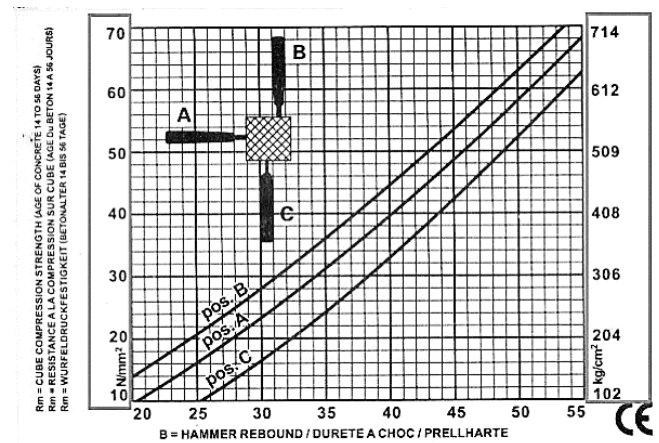


Figure 5 Relationship between the strength of concrete and reflection value (User Manual for Concrete Test Hammer PCE-HT-225A)

tion of reinforcing steel from concrete by peeling off its cover (Figure 6). After the extraction process, area corrosion measurements were conducted on the extracted round steel bars. This was achieved by wrapping a clear plastic material around the surface of bars in a circular manner. Subsequently, a sketch was made on the surface of reinforcing bars using a permanent black marker

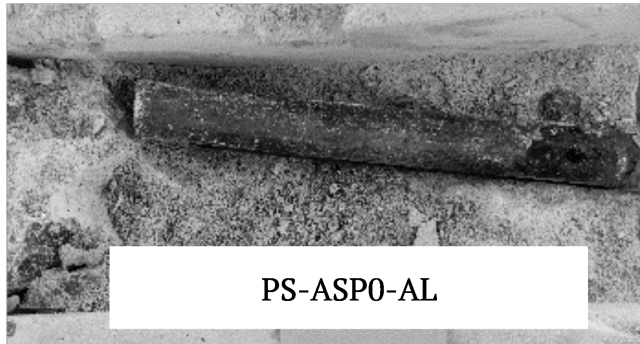


Figure 6 Visual inspection of reinforcing steel corrosion

to outline the areas affected by corrosion or rust. Computer image analysis software (Image J v1.49) was used to determine the corroded area of reinforcing steel (area corrosion). The software analyzes the marked areas on the surface of reinforcing bars to calculate the extent of corrosion. The inspection to confirm actual corrosion by extracting reinforcing steel from concrete specimen was conducted after 190 days from the initial detection of corrosion using the HCP measurement method.

3 RESULT

3.1 The HCP

The HCP values of the test specimens, as shown in Figure 7, exhibited a time-dependent change from 1 to 189 days. After the de-moulded process on the first day, the HCP values of all test specimens mixed with tap water and sea sand ranged from -100mV to -200mV . Conversely, specimens mixed with seawater and river sand displayed more negative potential values, ranging from -350mV to -450mV . These high negative values are attributed to the wetness of concrete and imperfect binding reaction to the cement (Dasar et al., 2016). Based on the changing time, potential values of all specimens gradually became more positive. The HCP values continued to recover, indicating that there was no corrosion in 90% of the specimens even after the cement hydration period at the age of 28 days. This trend suggested a perfect bond formation in the cement. Figure 7 also showed that at the age of 105 days, potential value of the PS-ASP0-AL specimen started to gradually decrease and continued to decline until the age of 189 days. Other specimens experienced a decrease in potential value at the age of 161 days, followed by a gradual decline until the age of 189 days. A total of

6 specimens with a very negative value below -256mV and a 90% probability of corrosion.

Figure 8 shows the HCP value of the specimen at the age of 189 days. Analysis of the figure revealed several notable observations. It was observed that all specimens mixed with river sand and seawater, regardless of the variations in RHA addition (ranging from 0% to 15%), exhibited potential values more negative or less than -256mV . This indicated a 90% probability of corrosion in these specimens. Furthermore, the test specimens mixed with sea sand, tap water and the addition of 10% and 15% RHA also showed a more negative potential value of -256mV , suggesting a 90% likelihood of corrosion. While the specimen mixed with sea sand and tap water, with no RHA addition (0% RHA), showed potential value of -166mV , indicating that 90% had not been corroded. The specimen mixed with sea sand and tap water, along with a 5% RHA addition, showed potential value of -55mV , suggesting a 50% risk of possible corrosion. From Figure 8, it was also found that the higher the substitution of RHA, the more negative potential value. This could be attributed to factors such as reduced water availability for cement hydration, delayed cement hydration, decreased OH^- content on the surface of RHA particles, and hindered transfer of Ca^{+2} from particle surfaces to the solution. Potential value of some specimens experienced a temporary recovery before decreasing again to a more negative potential.

3.2 Hammer Test

Once corrosion was detected in several specimens using the HCP method, a compressive strength test (hammer test) was conducted simultaneously at the age of 189 days. The results of the hammer test measurement at this stage, corresponding to each percentage of RHA substitution and using sea sand or river sand mixed with seawater and tap water, are shown in Table 6.

Blends of RHA and cement exhibit a more intricate hydration process compared to traditional pozzolanic materials. This complexity arises from the porous structure of RHA, which enables the adsorption and release of water. The interaction between RHA and cement hydration involves multiple factors, including the dilution impact, as well as chemical and internal curing effects (Park et al.,

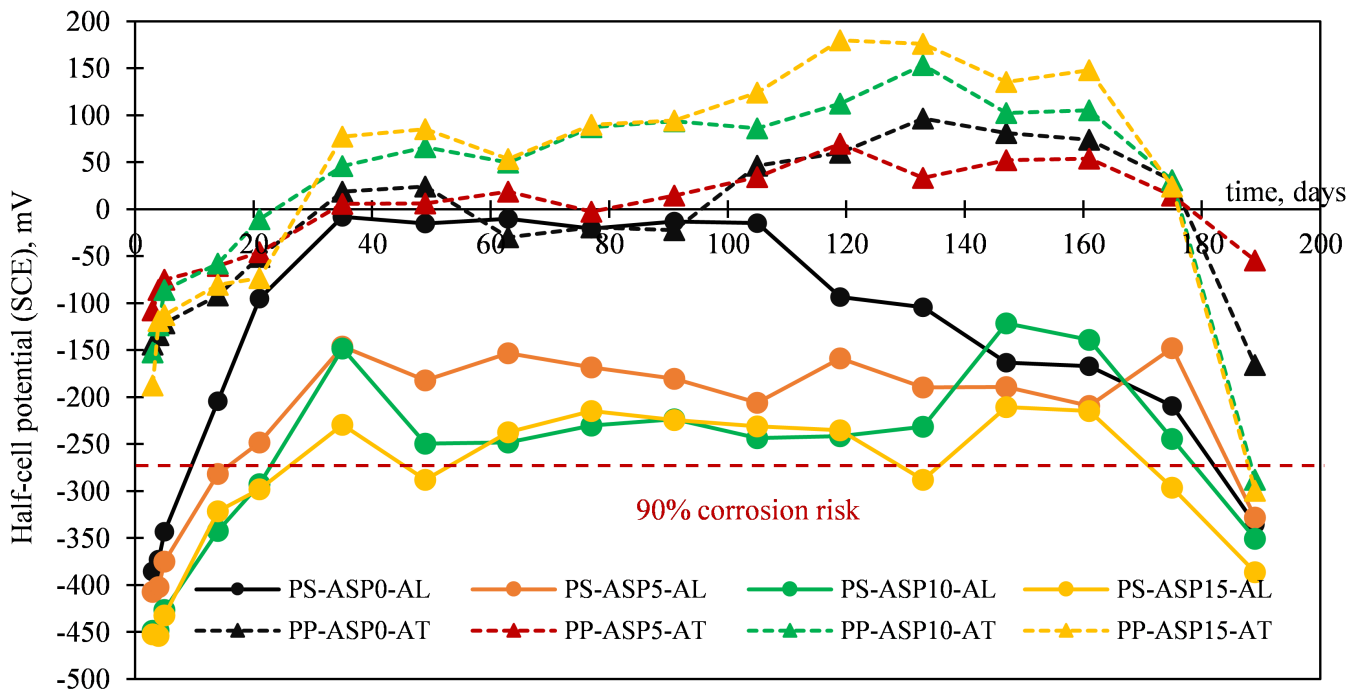


Figure 7 Time-dependent change of the HCP

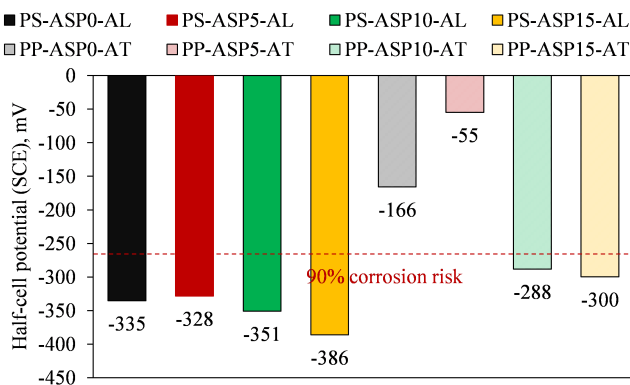


Figure 8 The HCP value at the age of 189 days

2016). The dilution effect is responsible for the reduction in cement content, while internal curing stems from the continual release of water from RHA, thereby promoting cement hydration. Additionally, the chemical effect refers to the pozzolanic interaction between SiO₂ and calcium hydroxide (CH) (Wang and Lee, 2009, 2010). As the relative humidity within the matrix declines, water is released from the pores of RHA particles, leading to the enhanced hydration of surrounding cement particles (Nguyen et al., 2010). This phenomenon significantly impacts the compressive strength of RHA-containing concrete. Based on Table 6, it was observed that specimens mixed with seawater, river sand and varying RHA additions, exhibited a higher compressive strength

Table 6. Compressive strength (Hammer test)

Term	Compressive strength (MPa)		Ratio of 189 days/28 days,%
	28-days	189- days	
PS-ASP0-AL	31	36	116.13
PS-ASP5-AL	25	40	160.00
PS-ASP10-AL	25	43	172.00
PS-ASP15-AL	26	38	146.15
PP-ASP0-AT	34	42	123.53
PP-ASP5-AT	31	38	122.58
PP-ASP10-AT	31	41	132.26
PP-ASP15-AT	28	34	121.43

ratio at 189 days compared to 28 days, in contrast to the specimen mixed with tap water, sea sand and varying RHA additions. The compressive strength ratios of 189 days and 28 days for PS-ASP5-AL, PS-ASP10-AL, and PS-ASP15-AL were 160%, 172% and 146.15%, respectively. The ratios for PP-ASP5-AT, PP-ASP10-AT, and PP-ASP15-AT were 122.58%, 132.26% and 121.43%, respectively. These results indicate that concrete mixed with seawater requires more time to improve its compressive strength. According to Otsuki et al. (2011), the compressive strength of seawater concrete in the long term is slightly higher compared to tap water concrete. This suggested that the presence of seawater in concrete mix can delay the hydration reaction of the cement, resulting in a longer time for the compressive strength to be

firm. Patah (2019) also reported that seawater-mixed concrete showed 10 MPa greater strength than tap water at a later age, with a compressive strength ratio of seawater to tap water of 1.2 after 36 years of reinforced concrete usage. Concrete incorporating RHA-15%, whether mixed with seawater or sea sand, showed the lowest compressive strength. This could be attributed to the characteristics of RHA used in the present study, particularly its white appearance. The moisture absorption capacity of white RHA is stronger than that of partially burned black RHA. The hydration of cement in concrete is insufficient, resulting in its reduced strength.

3.3 Actual Corrosion

Figure 9 shows actual inspection of corrosion on reinforcing steel that has been extracted from concrete. Based on visual observation, it is evident that the PS-ASP15-AL specimen has a considerably larger corrosion area compared to the PP-ASP15-AT. In order to calculate corrosion area, the extracted reinforcing bars were marked, and the extent of rust on its surface was measured.

Furthermore, Figure 10 shows the total corrosion observed at the age of 189 days for each specimen. The analysis of Figure 10 showed that all test specimens, which were mixed with seawater and river sand, exhibited corrosion. Corrosion areas were recorded as 15.67%, 14.54%, 35.85%, and 30% for varying RHA additions of 0%, 5%, 10%, and 15% respectively. The specimens mixed with tap water, sea sand and RHA additions of 10% and 15% displayed corrosion areas of 9.00% and 8.22%, respectively. Corrosion value of this area correlates with the HCP value in each specimen, which indicates a high corrosion risk category or 90% corrosion probability. The specimens mixed with tap water, sea sand and RHA additions of 0% and 5% showed no signs of corrosion with corrosion area of 0%. This observation aligns with the HCP values, indicating a low corrosion risk category with a 90% possibility of no corrosion. Based on this study, it was concluded that the partial replacement of cement with RHA-5% can be used simultaneously with seawater in concrete mixing. The larger corrosion area observed in specimens mixed with seawater compared to sea sand was attributed to the significant presence of free chlorides in sea-

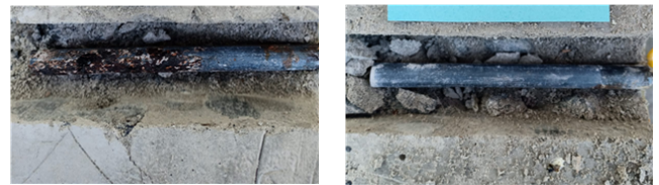


Figure 9 Actual corrosion of steel

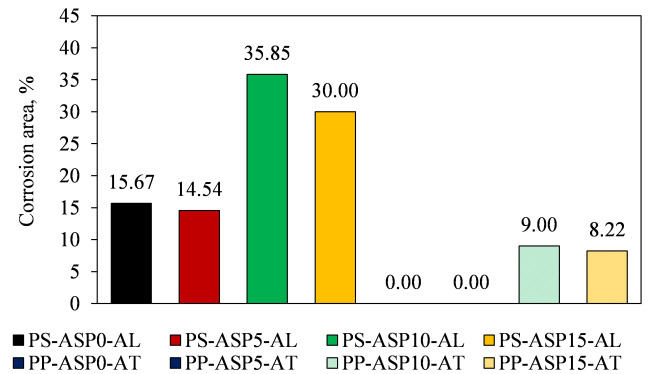


Figure 10 Corrosion area of steel

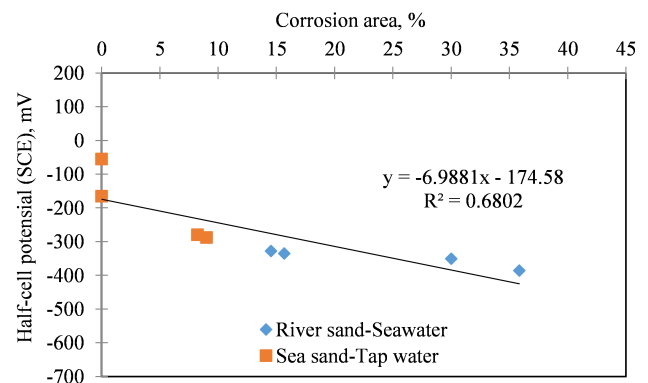


Figure 11 Relationship between the HCP with Corrosion area

water. The use of such water in concrete mixing and curing tend to result in a higher concentration of chloride ions coming into contact with reinforcing bars within a short period.

4 DISCUSSION

The relationship between the HCP value and actual corrosion of reinforcing steel is shown in Figure 11. However, the data suggested that the linear relationship between the electrochemical tests conducted using the HCP method and the observed corrosion is relatively weak. Equation (1) was used to determine the relationship between the HCP and actual corrosion.

$$y = -6.9881x - 174.58 \quad (1)$$

where x is the HCP value in mV and y is corrosion area in %. Figure 11 shows the linear relationship between the HCP method and actual corrosion has an R^2 -value of 0.6802. This indicates that further refinement is required to increase the accuracy of detecting potential corrosion in reinforcing bars when inspecting concrete with 0-15% RHA substitution combined with seawater and sea sand. When Figure 11 was analyzed, it was observed that all specimens mixed with river sand and sea water exhibited potential values greater than -300 mV, with corrosion area ranging from 0 to 10%. Meanwhile, all specimens mixed with sea sand and tap water exhibited potential values less than -300 mV, accompanied by larger corrosion areas within the range of 15 to 35%. This implied that corrosion observed in the specimen mixed with sea sand and tap water was significantly more severe, indicating low durability. The reduction in resistance to chloride-contaminated concrete, particularly in specimens with excessive RHA substitution (10% and 15%), was attributed to a decrease in C-S-H due to reduced cement content and sluggish pozzolanic reactions caused by increased water absorption. This is because RHA internal curing effect and pozzolanic reaction facilitate cement hydration, especially in the later stages, gradually reducing the porosity of the matrix and enhancing resistance to chloride ion penetration (Salas et al., 2009; De Sensale, 2010).

Chloride ions contribute to water scarcity by reducing the amount needed for further cement hydration. The final cement hydration reaction usually takes longer, leading to notable corrosion in specimens with RHA-10% and RHA-15%, particularly in the presence of chloride ions. RHA produced under specific circumstances contains a significant quantity of amorphous SiO_2 (Rashid et al., 2010), which exhibits some pozzolanic activity. The pozzolanic reaction of RHA promotes the production of more C-S-H gels and reduces the concentration of calcium hydroxide (CH) (Mehta and Monteiro, 2014). The presence of RHA particles redistributes water in the pores, playing a role in internal curing (Van et al., 2011). According to Saraswathy and Song (2007) and Salas et al. (2009), the internal curing effect enhances the strength and matrix growth of cement as well as improves

resistance to corrosion from sulfates, carbonation, and other agents while also promoting additional cement hydration.

5 CONCLUSION

The electrochemical measurements conducted on the test specimens, mixed with seawater, river sand, and different amounts of RHA (0%, 5%, 10%, and 15%), revealed that reinforcing steel in all specimens experienced corrosion using the HCP method. These findings align with the results obtained from the assessment of actual corrosion. Furthermore, it was concluded that the simultaneous use of tap water, sea sand and 5%-RHA in concrete mixing not only increased the compressive strength but also reduced the risk of corrosion, making it comparable to normal concrete. This implied that RHA contributed positively to enhancing the durability of concrete against corrosion. Future studies should investigate the application of RHA in reinforced concrete exposed to marine environments.

DISCLAIMER

The authors declare no conflict of interest.

AVAILABILITY OF DATA AND MATERIALS

All data are available from the author.

REFERENCES

- Boateng, A. and Skeete, D. (1990), 'Incineration of rice hull for use as a cementitious material: The guyana experience', *Cement and Concrete Research* 20(5), 795–802.
- Bui, D. (2001), 'Rice husk ash is a mineral admixture for high-performance concrete'.
- Dasar, A., Hamada, H., Sagawa, Y. and Irmawaty, R. (2013), Corrosion evaluation of reinforcing bar in seawater mixed mortar by electrochemical method, in 'Proceedings of the Japan Concrete Institute', Vol. 35, Nagoya, Japan, pp. 889–894.
- Dasar, A., Hamada, H., Sagawa, Y. and Yamamoto, D. (2016), 'Recovery in mix potential and polarization resistance of steel bar in cement hardened

matrix during early age of 6 months-sea-water mixed’.

Dasar, A., Patah, D., Hamada, H., Sagawa, Y. and Yamamoto, D. (2020), ‘Applicability of seawater as a mixing and curing agent in 4-year-old concrete’, *Construction and Building Materials* **259**, 119692.

De Sensale, G. (2010), ‘Effect of rice-husk ash on the durability of cementitious materials’, *Cement and Concrete Composites* **32**(9), 718–725.

Etxeberria, M., Fernandez, J. M. and Limeira, J. (2016), ‘Secondary aggregates and seawater employment for sustainable concrete dyke blocks production: Case study’, *Construction and Building Materials* **113**, 586–595.

Fapohunda, C., Akinbile, B. and Shittu, A. (2017), ‘Structure and properties of mortar and concrete with rice husk ash as partial replacement of ordinary portland cement—a review’, *International Journal of Sustainable Built Environment* **6**(2), 675–692.

Fu, Q., Wu, Y., Zhang, N., Hu, S., Yang, F., Lu, L. and Wang, J. (2020), ‘Durability and mechanism of high-salt resistance concrete exposed to sewage-contaminated seawater’, *Construction and Building Materials* **257**, 119534.

Gursel, A., Maryman, H. and Ostertag, C. (2016), ‘A life-cycle approach to environmental, mechanical, and durability properties of “green” concrete mixes with rice husk ash’, *Journal of Cleaner Production* **112**, 823–836.

Hammond, G. and Jones, C. (2008), ‘Embodied energy and carbon in construction materials’, *Proceedings of the Institution of Civil Engineers–Energy* **161**(2), 87–98.

Henry, C. and Lynam, J. (2020), ‘Embodied energy of rice husk ash for sustainable cement production’, *Case Studies in Chemical and Environmental Engineering* **2**, 100004.

Kishore, R., Bhikshma, V. and Prakash, P. (2011), ‘Study on strength characteristics of high-strength rice husk ash concrete’, *Procedia Engineering* **14**, 2666–2672.

Li, P., Li, W., Yu, T., Qu, F. and Tam, V. (2020), ‘Investigation on early-age hydration, mechanical properties and microstructure of seawater sea

sand cement mortar’, *Construction and Building Materials* **249**, 118776.

Li, Q., Geng, H., Shui, Z. and Huang, Y. (2015), ‘Effect of metakaolin addition and seawater mixing on the properties and hydration of concrete’, *Applied Clay Science* **115**, 51–60.

Mehta, P. and Monteiro, P. (2014), *Concrete: microstructure, properties, and materials*, McGraw-Hill Education.

Nguyen, V., Guang, Y., Klaas, V., Alex, L. and Danh, D. (2011), ‘The study of using rice husk ash to produce ultra-high-performance concrete’, *Construction and Building Materials* **25**(4), 2030–2035.

Nguyen, V., Guang, Y., Klaas, V., Zhanqi, G. and Danh, D. (2010), Hydration process of rice husk ash and silica fume in cement paste by means of isothermal calorimetry, in ‘The 6th International Conference on Concrete under Severe Conditions Environment and Loading’, Yucatan, Mexico, pp. 1521–1528.

Otsuki, N., Saito, T. and Tadokoro, Y. (2011), Possibility of seawater as mixing water in concrete, in ‘36th Conference on Our World in Concrete Structures’, Vol. 36, Singapore, pp. 131–138.

Park, K., Kwon, S. and Wang, X. (2016), ‘Analysis of the effects of rice husk ash on the hydration of cementitious materials’, *Construction and Building Materials* **105**, 196–205.

Patah, D. and Dasar, A. (2022), Strength performance of concrete using rice husk ash (rha) as supplementary cementitious material (scm), in ‘Journal of The Civil Engineering Forum’, pp. 261–276.

Patah, D., H. H. S. Y. . Y. D. (2019), ‘The effect of seawater mixing on corrosion of steel bar in 36-years old rc beams under marine tidal environment’, *Proceedings of the Japan Concrete Institute* **41**(1), 791–796.

Rashid, M., Molla, M. and Ahmed, T. (2010), ‘The durability of mortar in the presence of rice husk ash’, *Pan* **100**(41.5), 493–495.

Reddy, B. and Jagadish, K. (2003), ‘Embodied energy of common and alternative building materials and technologies’, *Energy and Buildings* **35**(2), 129–137.

- Salas, A., Delvasto, S., de Gutierrez, R. and Lange, D. (2009), 'Comparison of two processes for treating rice husk ash for use in high-performance concrete', *Cement and Concrete Research* **39**(9), 773–778.
- Saraswathy, V. and Song, H. (2007), 'Corrosion performance of rice husk ash blended concrete', *Construction and Building Materials* **21**(8), 1779–1784.
- Sikora, P. a. (2020a), 'The effects of seawater and nano silica on the performance of blended cement and composites', *Applied Nanoscience* **10**(12), 5009–5026.
- Sikora, P. a. (2020b), 'The effects of seawater on the hydration, microstructure and strength development of portland cement pastes incorporating colloidal silica', *Applied Nanoscience* **10**(8), 2627–2638.
- Ting, M., Wong, K., Rahman, M. and Joo, M. (2020), 'Mechanical and durability performance of marine sand and seawater concrete incorporating silico-manganese slag as coarse aggregate', *Construction and Building Materials* **254**, 119195.
- Van Tuan, N., Ye, G., Van Breugel, K., Fraaij, A. L. and Dai Bui, D. (2011), 'The study of using rice husk ash to produce ultra high performance concrete', *Construction and Building Materials* **25**(4), 2030–2035.
- Wang, X. and Lee, H. (2009), 'A model for predicting the carbonation depth of concrete containing low-calcium fly ash', *Construction and Building Materials* **23**(2), 725–733.
- Wang, X. and Lee, H. (2010), 'Modeling the hydration of concrete incorporating fly ash or slag', *Cement and Concrete Research* **40**(7), 984–996.
- Wang, Z., Zhao, X., Xian, G., Wu, G., Raman, R., Al-Saadi, S. and Haque, A. (2017), 'Long-term durability of basalt- and glass-fibre reinforced polymer (bfrp/gfrp) bars in seawater and sea sand concrete environment', *Construction and Building Materials* **139**, 467–489.
- Yu, C., Wu, Q. and Yang, J. (2017), 'Effect of seawater for mixing on properties of potassium magnesium phosphate cement paste', *Construction and Building Materials* **155**, 217–227.

[This page is intentionally left blank]